

# Solving Open Polygons in Elastic Correction of Dead-Reckoning Errors

MATTEO GOLFARELLI, STEFANO RIZZI  
DEIS, University of Bologna  
Viale Risorgimento, 2 - 40136 Bologna  
ITALY

**Abstract:** - A major problem in map building is due to the imprecision of sensor measures. In a previous paper we proposed a technique, called elastic correction, for correcting the dead-reckoning errors made during the exploration of an unknown environment by a robot capable of identifying landmarks. Elastic correction is based on an analogy between the relational graph modelling the environment and a mechanical structure: the map is regarded as a truss where each route is an elastic bar and each landmark a node; errors are corrected as a result of the deformations induced from the forces arising within the structure as inconsistent measures are taken. The main weakness of this method lies in the way positional inconsistencies are solved when routes are covered for the first time. In this paper we improve first-sight elastic correction by replacing the heuristics previously adopted with a new approach which considers all the knowledge of the surrounding map acquired so far; this is achieved by calculating the minimum forces to be applied in order to restore metric consistency. The effectiveness of the new approach is demonstrated by presenting some experimental tests.

**Key-Words:** - Correction of Positional Error, Dead-Reckoning, Map Building, Self-Positioning, Structural Analysis, Structured Environments

## 1 Introduction

Most mobile robots need a map of the environment to carry out successfully the navigational tasks assigned to them. Several techniques for environment representation have been devised in the literature [7] [13] [8]. Though in some applications a detailed map of the environment is given to the robot a priori, map building is still an important issue for all the applications in which the environment is unknown and, in general, in order to have a robot exhibit a fully autonomous behaviour.

Building an accurate map of the environment is made complex by the imprecision of measurements, which produces metric errors. In particular, we are interested in systematic errors which can be modelled by a probabilistic distribution (dead-reckoning errors); they are inherently associated to every sensor, thus they play a significant role in determining the global error.

In [6] we proposed an original approach to map building, called *elastic correction*, which can be applied to correct the dead-reckoning errors made by a robot navigating within an environment where landmarks are present. The environment is modelled by a relational graph whose vertices and arcs represent, respectively, the landmarks sensed and the inter-landmark routes experienced [10]. While exploring the environment, the robot calculates the relative position of each landmark

compared to the one met immediately before, by applying dead-reckoning; when it meets a landmark it has already seen, self-positioning and error correction are achieved together by combining the new measurements collected with the knowledge accumulated so far. In particular, elastic correction is based on an analogy between the graph modelling the environment and a mechanical structure: the map is regarded as a truss where each route is an elastic bar and each landmark a node. Errors are corrected as a result of the deformations induced by the forces arising within the structure as inconsistent measurements are taken. The elasticity parameters characterizing the structure are used to model the uncertainty on odometry.

The main weakness of elastic correction lies in the way positional inconsistencies are solved when routes are covered for the first time (*first-sight correction*). In fact, the method proposed in [6] is based on a heuristic criterion which does not fully exploit the knowledge acquired so far. On the other hand, first-sight correction has a crucial role in determining the overall results because (1) the map metrics should be well assessed since the very first steps of exploration and (2) in real world applications, it may not be possible to cover repeatedly the same routes.

In this paper we improve first-sight correction by replacing the heuristics previously adopted with a new approach which considers all the knowledge

acquired so far. This is achieved by calculating the minimum forces to be applied to the whole map in order to restore metric consistency.

## 2 Pose estimation

Let the *pose* of the robot at time step  $k$  be expressed by its position in a Cartesian plane,  $\mathbf{p}^{(k)} = \begin{bmatrix} x^{(k)} \\ y^{(k)} \end{bmatrix}$ , and by its orientation,  $\varphi^{(k)}$ ; the well-known dead-reckoning formula determines the pose at step  $k+1$  as a function of the pose at step  $k$  and of the moduli of the linear and angular velocities,  $w^{(k+1)}$  and  $u^{(k+1)}$ , respectively, measured by sensors at step  $k+1$ :

$$\begin{aligned} \mathbf{p}^{(k+1)} &= \begin{bmatrix} x^{(k)} + T w^{(k+1)} \cos \varphi^{(k)} \\ y^{(k)} + T w^{(k+1)} \sin \varphi^{(k)} \end{bmatrix}, \\ \varphi^{(k+1)} &= \varphi^{(k)} + T u^{(k+1)} \end{aligned} \quad (1)$$

where  $T$  is the sampling interval of sensors. Using this formula, the errors made in measuring the angular velocity  $u^{(k+1)}$  accumulate through all the subsequent evaluations of the pose.

On the other hand, if the robot mounts a compass, while the new coordinates  $x^{(k+1)}$  and  $y^{(k+1)}$  are still calculated as above,  $\varphi^{(k+1)}$  may be measured directly; thus, each new positional estimate is not affected by the errors made in measuring the robot's orientation at the previous steps and the measurements relative to distinct routes are independent from each other.

An estimate of the positional uncertainty for a robot moving along a path can be calculated starting from the density function  $\delta(x, y, \mathbf{C}^{(k)})$ , expressing

the probability that the true robot position is  $\mathbf{p} = \begin{bmatrix} x \\ y \end{bmatrix}$  instead of the measured position  $\mathbf{p}^{(k)}$ . The covariance matrix  $\mathbf{C}^{(k)}$  depends on the features of the sensors mounted on the robot. While from a theoretic point of view every density function is possible, previous experiences [14] [9] show that the errors can be effectively modelled using a Gaussian distribution with null mean. The area in which the robot may stand with non-negligible probability is an ellipse whose shape and dimensions depend on the length and complexity of the path [1].

It is well known that the behaviour of compasses is strongly affected by the proximity of metallic objects, which is quite common in indoor environments. This problem can be faced by comparing the positional estimate based on the compass with that calculated by odometer-based dead-reckoning: errors due to metallic objects will be detected when the estimated orientations suddenly become significantly conflicting; in this case, the covariance matrix for conventional dead-

reckoning can be used to compute  $\delta$ .

## 3 Elastic correction

The map built by the robot is structured as a non-directed graph  $\mathcal{M}=(V, R)$ . Each vertex  $v_i \in V$  represents a landmark sensed and is labelled with its

estimated position  $\mathbf{p}_i = \begin{bmatrix} x_i \\ y_i \end{bmatrix}$ ; arc  $r_{ij} \in R$  represents the route connecting  $v_i$  and  $v_j$  and is labelled with the number of times the route has been covered so far,  $t_{ij}$ . We will denote by  $\vartheta_{ij}$  (*route orientation*,  $0 \leq \vartheta_{ij} < \pi$ ) the absolute orientation of the segment connecting  $v_i$  to  $v_j$ , and by  $s_{ij}$  (*route stretch*) its length, calculated as the Euclidean distance between  $\mathbf{p}_i$  and  $\mathbf{p}_j$ . Every time the robot moves from  $v_i$  to  $v_j$  covering the corresponding route, the covariance matrix expressing the uncertainty induced on the position of  $v_j$  is calculated; the value of the covariance matrix depends on how long and winding is the route covered. Arc  $r_{ij}$  is labelled with the average of the  $t_{ij}$  covariance matrices calculated,  $\mathbf{C}_{ij}$ .

Elastic correction is performed during exploration in two phases. *First-sight correction* is carried out whenever a known landmark is met after covering one or more unknown routes. *Refinement correction* is performed when a known route is covered again.

We do not consider topological errors since we assume that the robot is capable of recognizing a landmark it has already met. Landmark recognition is a complex task; in order to achieve univocal identification, the imprecision inherent in sensory-based classification algorithms can be overcome by augmenting them with approximate metric information.

### 3.1 Environment modelling

Elastic correction is based on the analogy between the environment map  $\mathcal{M}$  and a pin-jointed truss whose elements and nodes represent, respectively, routes and landmarks (see Figure 1); the parameters defining the stiffness of each element when loaded sum up the characteristics of the corresponding route. The more elastic an element, the greater the change in length and orientation that it will experience when loaded; thus, stiffness should be proportional to the certainty on the stretch and orientation of the corresponding route.

An element representing a route  $r$  with stretch  $s$  and orientation  $\vartheta$  may be thought of as a bar long  $s$ , oriented according to  $\vartheta$  and behaving as follows:

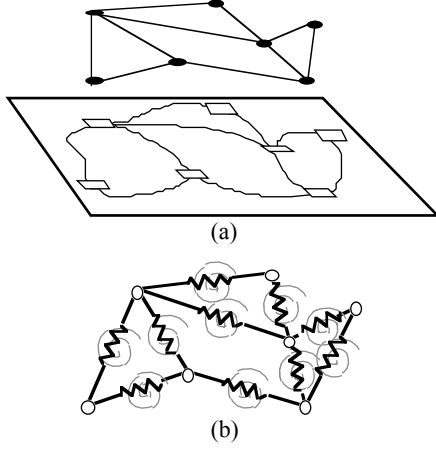


**Figure 1.** Graph-based representation of an environment (a) and equivalent truss (b).

- it can be compressed elastically along its axis to model uncertainty on the route stretch,  $s$ ;
- it can neither be bended nor twisted;
- it can rotate elastically to model uncertainty on the route orientation,  $\vartheta$ .

From a mechanical point of view, a bar with these characteristics can be modelled by combining a linear axial spring and a rotational spring (see Figure 2), whose spring constants  $k_a$  and  $k_r$  must be defined in function of the probability density function of the robot position. The details are given in [6].

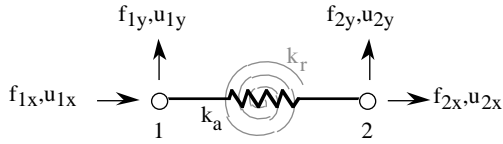


**Figure 2.** Truss basic element, including a linear elastic spring (in black) and a rotational elastic spring (in grey).

### 3.2 The stiffness method

Let an elastic structure which can be modelled as an assemblage of members connected at node points be given. The problem of determining the displacements of the nodes when one or more of them are loaded with a force can be solved by applying the *stiffness method* [11].

Let  $n$  be the number of nodes in an elastic bidimensional structure; the relationships linking the displacements of the nodes to the forces applied to them are expressed in matrix form by the *stiffness equation*:

$$\mathbf{u} = \mathbf{K}^{-1} \mathbf{f}$$

where  $\mathbf{f}$  is the column matrix of x- and y-components of the nodal forces,  $\mathbf{u}$  is the column matrix of the x- and y-components of the nodal

displacements, and  $\mathbf{K}$  is a symmetric square matrix with rank  $2n$  (*stiffness matrix*), whose elements are the stiffness coefficients of the structure.

In order to solve the stiffness equation, the  $n$  nodes may be partitioned in two sets  $\alpha$  and  $\beta$ , the first one including the free nodes, and the latter containing the nodes whose displacements are constrained. The relationship between displacements and forces can thus be rewritten as:

$$\begin{bmatrix} \mathbf{u}_\alpha \\ \mathbf{u}_\beta \end{bmatrix} = \begin{bmatrix} \mathbf{K}^{-1}_{\alpha\alpha} & \mathbf{K}^{-1}_{\alpha\beta} \\ \mathbf{K}^{-1}_{\beta\alpha} & \mathbf{K}^{-1}_{\beta\beta} \end{bmatrix} \begin{bmatrix} \mathbf{f}_\alpha \\ \mathbf{f}_\beta \end{bmatrix} \quad (2)$$

where  $\mathbf{f}_\alpha$  and  $\mathbf{f}_\beta$  represent, respectively, the loads applied to the free nodes and the reactions in the constrained nodes.

### 3.3 Correction of first-sight errors

Suppose the robot is exploring an unknown area starting from a known landmark  $v_0$  in position  $\mathbf{p}_0$ . It meets the unknown landmarks  $v_1, \dots, v_{m-1}$  by covering a sequence of unknown routes, and finally reaches a landmark  $v_m$  which it has already met. When  $v_m$  is reached, the new positional estimate  $\mathbf{p}''_m$  computed by dead-reckoning may be compared to the previous one,  $\mathbf{p}'_m$ ; due to sensor errors, the two estimates will certainly differ. Let

$$\bar{\mathbf{u}}_m = \mathbf{p}''_m - \mathbf{p}'_m$$

If  $v_m$  has been met before  $v_0$ , the segments orderly connecting  $\mathbf{p}_0$  to  $\mathbf{p}''_m$  form an open polygonal (see Figure 3.a). Otherwise, the segments orderly connecting  $\mathbf{p}'_m$  to  $\mathbf{p}''_m$  form a closed polygonal (see Figure 3.b).

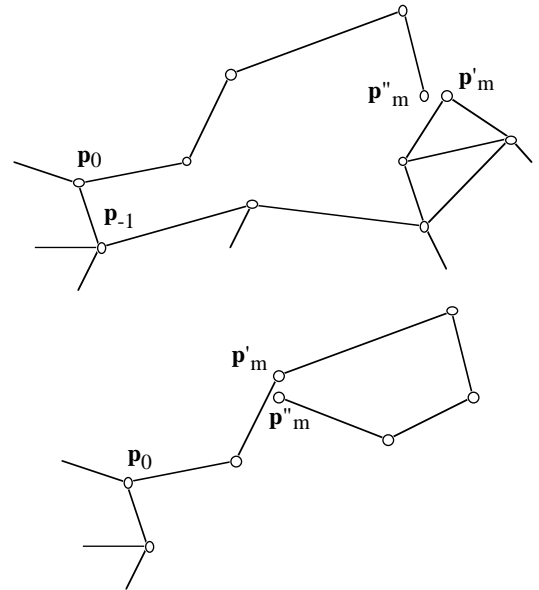


**Figure 3.** Error correction on open (top) and closed (bottom) polygonals.

The graph representing the environment should be metrically consistent at each time during exploration, hence, the two positional estimates for  $v_m$  must be forced to agree exactly. We assume the error on the stretch of each route to be proportional to the positional uncertainty induced by that route. In the solution proposed in [6], metrical correction was achieved as follows:

- constraining  $p_0$  and applying a displacement  $\bar{u}_m$  to  $p''_m$  if the polygonal is open;
- constraining  $p'_m$  and applying a displacement  $\bar{u}_m$  to  $p''_m$  if the polygonal is closed.

In both cases, the displacement applied moves  $p''_m$  on  $p'_m$  thus restoring the metric consistency of the graph; the displacements calculated for the free nodes determine the new positions for the landmarks involved.

Figure 4 shows an example for a simple closed polygonal.

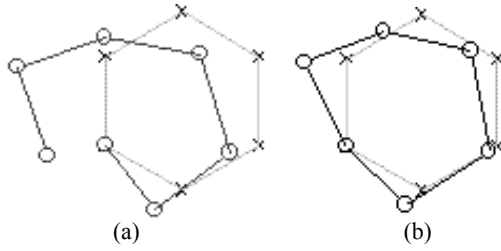


**Figure 4.** Elastic correction on a regular hexagon. The real graph is in light grey; the measured one in dark grey (a); the corrected one is in black (b).

### 3.4 Refinement of map measurements

Every time the robot covers a route  $r_{ij}$  it has covered before, it can exploit the new information acquired to improve the current estimate of the stretch and orientation of  $r_{ij}$  and, thus, that of the positions of its end landmark  $v_i$  and  $v_j$ . Reasonably, the estimates for  $r_{ij}$  should be equal, at each time, to the average of the data measured so far. The desired displacements for  $v_i$  and  $v_j$  are calculated by imaging to rotate  $r_{ij}$  around its midpoint in order to let it assume the new stretch and orientation.

This solution is not satisfactory since it does not take into account all the knowledge of the environment collected so far, while using global knowledge to correct the error on a single route is essential when the certainty on the routes is not evenly distributed. Another issue arising when correcting the error on a route is how metric consistency for the graph representing the environment is maintained: in fact, correcting the stretch and orientation of  $r_{ij}$  implies modifying the

stretches and orientations of the adjacent routes.

Our mechanical model allows both issues to be addressed. Let  $r_{ij}$  be the last route experienced. Firstly, the forces producing the desired displacements on the ends of  $r_{ij}$  are calculated on a reference structure including  $r_{ij}$  and the two adjacent routes of maximum stiffness. Then, these forces are applied to  $v_i$  and  $v_j$  within a structure including the set of routes connecting the  $\eta$  landmarks nearest to  $r_{ij}$ . Further details can be found in [6].

## 4 Solving open polygonals

The approach described in Section 3.3 for closed polygonals is correct since metric inconsistency is only due to the errors made by the robot while covering the path between  $v_h$  and  $v_m$ , and correction affects exactly the corresponding set of routes.

On the other hand, the solution adopted for open polygonals (which we will call *constrained stretch*, CS) represents a simplification since it assumes that the errors have been made inside the polygonal. On the contrary, for example, in Figure 3.a the path  $p_0, p_1, \dots, p''_m$  could be mostly correct while the positional inconsistency could derive mainly from the path  $p_0, p_{-1}, \dots, p'_m$ .

The approach we propose in this section, which we will call *minimum magnitude* (MM), removes the previous assumption and determines the optimal stretches to restore metric consistency by keeping all the information acquired so far into account, consistently with the solution adopted for map refinement. The improvement obtained is very relevant since, in real environments, the robot is often required to cover open polygonals.

Keeping the errors made outside the polygonal into account implies considering a surrounding area determined by the set of routes connecting the  $\eta$  landmarks nearest to  $v_m$ . The structure we define to model the problem includes all the landmarks belonging to this area; among these, the landmarks lying on the external border are constrained. Let  $\alpha$  and  $\beta$  be the sets of free and constrained nodes, respectively.

Restoring metric consistency requires both  $p'_m$  and  $p''_m$  (belonging to  $\alpha$ ) to be moved to the same position  $p^*_m$ . In order to accomplish this, an infinite number of couples of forces  $f', f''$  to be applied to  $p'_m$  and  $p''_m$  respectively could be used. All these couples satisfy the following linear system

$$A f = -\bar{u}_m \quad (3)$$

where  $\bar{u}_m = p''_m - p'_m$ ,  $f = \begin{bmatrix} f' \\ f'' \end{bmatrix}$  and  $A$  is a  $(2 \times 4)$

matrix obtained from  $\mathbf{K}^{-1}_{\alpha\alpha}$  assuming that the only forces applied to the truss are  $\mathbf{f}'$  and  $\mathbf{f}''$ . Within this infinite set, we choose the couple  $\mathbf{f}^*$ ,  $\mathbf{f}''^*$  with minimum magnitude. Intuitively, this choice produces the minimum truss deformation.

The problem of determining  $\mathbf{f}^*$  and  $\mathbf{f}''^*$  can be formulated as a constrained optimization problem where the function to be minimized is the norm of  $\mathbf{f}$  while the constraint is expressed by (3):

$$\begin{cases} \min(\|\mathbf{f}\|_2^2) = \min(\mathbf{f}^T \mathbf{f}) \\ \mathbf{A} \mathbf{f} = -\bar{\mathbf{u}}_m \end{cases} \quad (4)$$

This problem can be solved using the Lagrangian method [4]:

$$L(\mathbf{f}, \lambda) = \mathbf{f}^T \mathbf{f} - (\mathbf{A} \mathbf{f} + \bar{\mathbf{u}}_m)^T \lambda$$

determining the linear system:

$$\begin{cases} 2\mathbf{f} - \mathbf{A}^T \lambda = 0 \\ \mathbf{f}^T \mathbf{A}^T + \bar{\mathbf{u}}_m^T = 0 \end{cases}$$

that admits an analytic solution.

Figure 5.a shows the error made by the robot while covering an open polygon; in Figures 5.b and 5.c the inconsistency is solved by applying CS and MM, respectively. Figure 6 shows the corresponding forces for MM. It should be noted that the two forces have both different magnitudes and different directions; this is a consequence of the truss structure which induces different constraints on  $\mathbf{p}'_m$  and  $\mathbf{p}''_m$ .

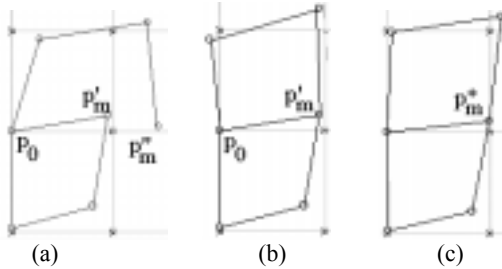


**Figure 5.** Open polygonal correction on a rectangular mesh. The real graph is in light grey; the measured one in dark grey (a). In (b) correction is achieved by CS, in (c) by MM.

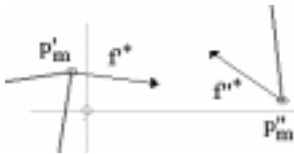


**Figure 6.** Forces applied to solve the open polygon in Fig. 5.

## 5 Experimental results and conclusion

We have extensively tested the elastic correction technique on a set of environments in order to

evaluate its effectiveness and robustness. We estimate the error on the map metric by two measurements: the average percentage error on the stretch of the routes,  $\sigma$ , and the average error on the orientation of the routes,  $\rho$ .

Table I and Figure 7 show the results of open polygonal correction on a regular map, assuming that both the variances of the odometer and compass errors are 0.09. It is remarkable how, as compared to CS, the MM approach not only restores map consistency but also significantly reduces the overall error.

	$\sigma$ (%)	$\rho$ (rad)
before correction	6.9	0.065
after correction with CS	6.9	0.059
after correction with MM	5.7	0.050

**Table I.** Errors for the first-sight correction in Figure 7.

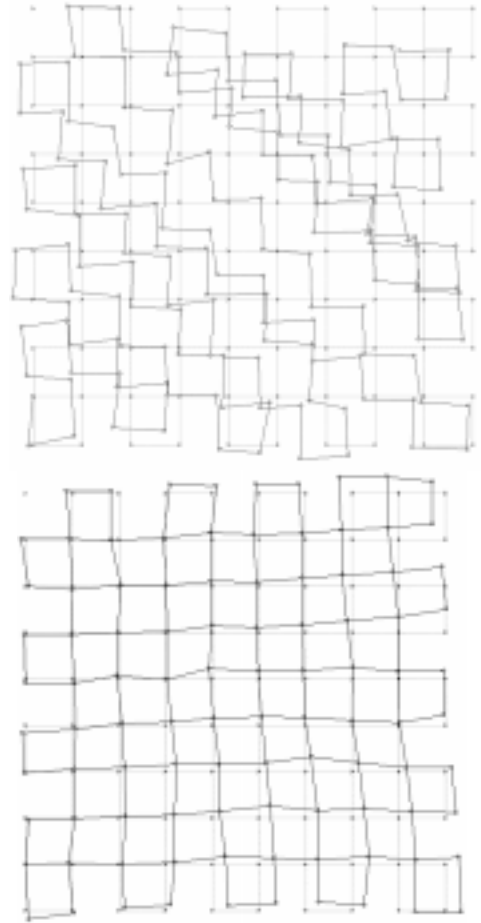


**Figure 7.** Open polygonal correction on a regular map. The real graph is in light grey, the measured one in dark grey (top), the one corrected with MM in black (bottom).

In order to prove the effectiveness of our technique, we compared it with the method proposed in [9] (which we will call ML) which operates on a graph-based environment representation and allows the global poses of multiple scans to be calculated by using all the pose

relations as constraints. The scan poses are considered as variables. A pose relation is an estimated spatial relation between the two poses which can be derived from matching two range scans. Global poses are then estimated by solving an optimization problem based on maximum likelihood.

The tests, whose results are shown in Table II, were made on an irregular dishomogeneous map which simulates a real-world environment. MM confirms to be superior to CS, and is comparable with ML. Our elastic correction technique turns out to be superior to ML when each route is experienced more than once. Figure 8 shows how, adopting elastic correction, the average errors on route stretch and orientation is significantly decreased as the map is repeatedly toured; on the contrary, after 10 tours, the average errors adopting ML increase to  $\sigma = 12.8\%$  and  $\rho = 0.135$ . This result can be explained considering that ML assumes that all the observation errors are mutually independent, while in elastic correction the deformation of each bar depends on the characteristics of the others.

	$\sigma$ (%)	$\rho$ (rad)
before correction	9.6	0.077
after correction with CS	9.5	0.081
after correction with MM	7.7	0.069
after correction with ML	7.5	0.073

**Table II.** Errors for the first-sight correction in Figure 7.

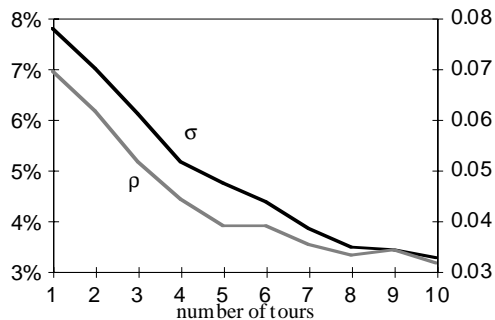


**Figure 8.** Errors on route stretch and orientation in function of the number of exploration tours.

The other correction approaches proposed in the literature are either based on assumptions and sensory equipment radically different from our and thus can hardly lead to a quantitative comparison [3] [12].

#### References:

[1] M. Adams *et al.*, Control and localisation of a post distributing mobile robot, *Int. Conf on Intelligent Robots and System*, Munich, 1994, pp. 150-156.

[2] S. Cooper, H. Durrant-Whyte, A Kalman filter for GPS navigation of land vehicles, *Proc. Int. Conf on Intelligent Robots and System*, Munich, 1994, pp. 157-163.

[3] S.P. Engelson, D. V. McDermott, Error correction in mobile robot map learning, *Proc. IEEE Int. Conf. On Robotics and Automation*, 1992.

[4] R. Fletcher, *Practical methods of optimization*, John Wiley & Sons, 1987.

[5] M. Golfarelli, D. Maio, S. Rizzi, A hierarchical approach to sonar-based landmark detection in mobile robots, *Proc. 5th Symp. on Intelligent Robotics Syst.*, Stockholm, Sweden, 1997, pp. 77-84.

[6] M. Golfarelli, D. Maio, S. Rizzi, Elastic Correction of Dead-Reckoning Errors in Map Building, *Proc. IEEE/RSJ Int. Conf. on Intelligent Robotic Systems (IROS'98)*, Victoria, Canada, 1998, pp. 905-911.

[7] D. Kortenkamp, T. Weymouth, Topological mapping for mobile robots using a combination of sonar and vision sensing, *Proc. AAAI'94*, 1994.

[8] J.J. Leonard, H.F. Durrant-Whyte, *Directed sonar sensing for mobile robot navigation*, Kluwer Academic Publ., 1992.

[9] F. Lu, E. Milios, Globally consistent range scan alignment for environment mapping, *Autonomous Robots*, vol. 4, 1997, pp. 333-348.

[10] D. Maio, D. Maltoni, S. Rizzi, Dynamic Clustering Of Maps In Autonomous Agents, *IEEE Trans. Pattern Analysis and Machine Intelligence*, vol. 18, n. 11, 1996, pp. 1080-1091.

[11] H.C. Martin, *Introduction to matrix methods of structural analysis*, McGraw-Hill, 1966.

[12] H. Shatkay, L.P. Kaelbling, Learning topological maps with weak local odometric information, *Proc. 15th Int. Joint Conf. on Artificial Intelligence*, Nagoya, 1997, pp. 920-927.

[13] S. Thrun, Learning metric-topological maps for indoor mobile navigation. *AI Journal*, vol. 99, n. 1, 1998, pp. 21-71.

[14] Y. Tonouchi, T. Tsubouchi, S. Arimoto, Fusion of dead-reckoned positions with a workspace model for a mobile robot by bayesian inference, *Proc. Int. Conf. on Intelligent Robots and System*, Munich, 1994, pp. 1347-1354.